Published in final edited form as:

Cell Chem Biol. 2018 August 16; 25(8): 941–951.e6. doi:10.1016/j.chembiol.2018.04.012.

Construction of Fluorescent Analogs to Follow the Uptake and Distribution of Cobalamin (Vitamin B_{12}) in Bacteria, Worms, and Plants

Andrew D. Lawrence[1,4], **Emi Nemoto-Smith**[1,2,4], **Evelyne Deery**[1], **Joseph A. Baker**[1], **Susanne Schroeder**[1], **David G. Brown**[1], **Jennifer M.A. Tullet**[1], **Mark J. Howard**[1], **Ian R. Brown**[1], **Alison G. Smith**[3], **Helena I. Boshoff**[2], **Clifton E. Barry III**[2], and **Martin J. Warren**[1,5,*]

[1]School of Biosciences, University of Kent, Canterbury, Kent CT2 7NJ, UK

[2]National Institute of Allergy and Infectious Diseases, National Institutes of Health, Bethesda, MD 20850, USA

[3]Department of Plant Sciences, University of Cambridge, Downing Street, Cambridge CB2 3EA, UK

[4]These authors contributed equally

[5]Lead Contact

SUMMARY

Vitamin B_{12} is made by only certain prokaryotes yet is required by a number of eukaryotes such as mammals, fish, birds, worms, and Protista, including algae. There is still much to learn about how this nutrient is trafficked across the domains of life. Herein, we describe ways to make a number of different corrin analogs with fluorescent groups attached to the main tetrapyrrole-derived ring. A further range of analogs were also constructed by attaching similar fluorescent groups to the ribose ring of cobalamin, thereby generating a range of complete and incomplete corrinoids to follow uptake in bacteria, worms, and plants. By using these fluorescent derivatives we were able to demonstrate that *Mycobacterium tuberculosis* is able to acquire both cobyric acid and cobalamin analogs, that *Caenorhabditis elegans* takes up only the complete corrinoid, and that seedlings of higher plants such as *Lepidium sativum* are also able to transport B_{12}.

In Brief

*Correspondence: m.j.warren@kent.ac.uk.

AUTHOR CONTRIBUTIONS

A.D.L., E.N.-S., E.D., J.A.B., and S.S. all undertook aspects of the experimental work including cloning, protein purification, and synthesis, and helped with the interpretation of the data. D.G.B. collected the X-ray data and assisted A.D.L. and E.N.-S. with the structure determination of CobH. M.J.H. performed all NMR data acquisition and assisted A.D.L. with analyses. J.M.A.T., E.D., and E.N.-S. designed the *C. elegans* experiments. A.G.S. helped in the design of the plant-based investigations. I.R.B. undertook some of the imaging experiments and provided guidance on experiment design. H.I.B. and C.E.B. designed the TB work. A.D.L., E.D., E.N.-S., and M.J.W. designed the experiments and wrote the paper.

SUPPLEMENTAL INFORMATION

Supplemental Information includes six figures and two tables and can be found with this article online at https://doi.org/10.1016/j.chembiol.2018.04.012.

DECLARATION OF INTERESTS

The authors declare no competing interests.

Lawrence et al., employed chemical biology approaches to construct a range of fluorescent vitamin B_{12} derivatives. They demonstrated that these fluorescent variants can be used to follow intracellular B_{12} trafficking in bacteria, including *E. coli* and *M. tuberculosis*, the worm *C. elegans*, and a higher plant (*Lepidium sativum*).

Graphical Abstract

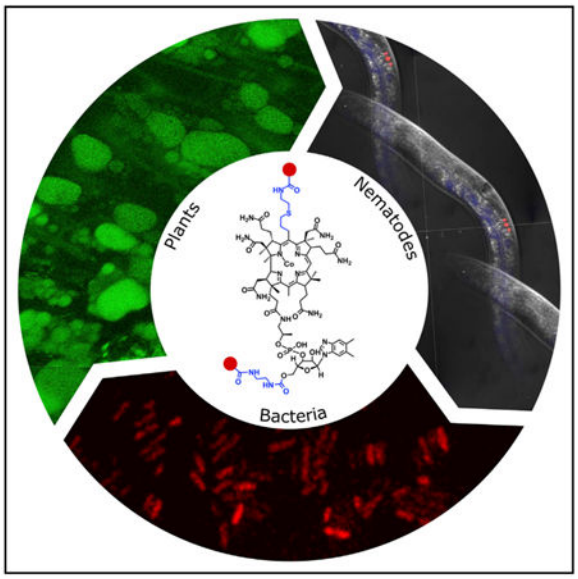

INTRODUCTION

The cobamides encompass a group of closely structurally related nutrients, cofactors, and coenzymes that harbor a cobalt-containing corrin ring, and are often loosely referred to as vitamin B_{12} (Figure 1) (Renz, 1999; Warren et al., 2002). These molecules vary in the nature of the upper ligand attached to the cobalt and the character of the lower nucleotide loop. Cobalamin, for instance, contains dimethylbenzimidazole as the base in the nucleotide loop but this is replaced with adenine in pseudocobalamin (Figure 1) (Degnan et al., 2014; Maggio-Hall and Escalante-Semerena, 2003). In the biologically active forms of cobalamin the cobalt ion is normally either adenosylated (adenosylcobalamin) or methylated (methylcobalamin) (Banerjee and Ragsdale, 2003), while vitamin B_{12} represents the cyanolated derivative of cobalamin that is produced during the commercial extraction and isolation of the nutrient (Martens et al., 2002). However, the term B_{12} is frequently used to refer to all forms of cobalamin.

Cobamides are produced exclusively by certain prokaryotes (Roth et al., 1996). Apart from cobalamin and pseudocobalamin, further variants with shorter nucleotide chain lengths and/or alternative nucleotide bases are synthesized by different bacteria (Degnan et al., 2014; Krautler et al., 2003; Renz, 1999). Cobamides are made via either an anaerobic or an aerobic biochemical pathway, both involving around 30 enzyme-mediated steps (Blanche et al., 1995; Deery et al., 2012; Moore et al., 2013; Warren et al., 2002). The key steps of the aerobic pathway are shown in Figure 1, which concisely depicts contraction of the

tetrapyrrole ring, insertion of the cobalt ion, and building of the nucleotide loop. Variations in the construction of the lower nucleotide loop, mediated by different substrate preferences for bases and linkers (Figure 1) during its biosynthesis, give rise to the assorted cobamides that are found in nature (Chan and Escalante-Semerena, 2011; Crofts et al., 2013; Krautler et al., 2003; Maggio-Hall and Escalante-Semerena, 2003; Zayas et al., 2007). Many prokaryotic microorganisms (Allen and Stabler, 2008; Degnan et al., 2014; Gray and Escalante-Semerena, 2009) and microbial eukaryotes (Croft et al., 2005; Helliwell et al., 2016) rely on other producers of cobamides, where both bacteria and archaea can be counted, and therefore have to recover the nutrient from the environment they inhabit. Such salvage systems often involve remodeling of the lower nucleotide loop to produce the corrin variant that suits the new host.

In this respect bacteria, as well as archaea, can be divided into a range of classes with regard to their B_{12} requirements. There are bacteria that make their own cobalamin, those that are auxotrophic for the nutrient, those that require cobalamin for some non-essential processes, and those that do not require the nutrient at all. In this way the nutrient plays an important role in bacterial ecology, especially in complex microbial communities (Degnan et al., 2014; Helliwell et al., 2016). However, little is known about the movement of cobamides in such communities, whether it is specifically shared or exchanged in mutualistic or symbiotic relationships.

Bacteria are also the source of cobalamin for a large number of eukaryotes that require the nutrient for either specific methylation or isomerization reactions. For instance, approximately 50% of all microalgal species require cobalamin for growth, and it has been shown that bacteria can provide this compound in course of a symbiotic exchange for photosynthate (Croft et al., 2005). Similarly, enteric bacteria are the source of cobalamin (Roth et al., 1996) in ruminants such as cattle and, as dairy products and meat represent a major form of human dietary cobalamin, and are therefore also responsible for most of the cobalamin found in humans (Brito et al., 2015; Girard et al., 2009). Other eukaryotes, including nematode worms (Yilmaz and Walhout, 2014), fish (Greibe et al., 2012), and birds (Zaman and Zak, 1989) have to acquire cobalamin as part of their diets from B_{12}-producing bacteria. Within eukaryotic cells cobalamin is further compartmentalized, with methylcobalamin found in the cytoplasm associated with methionine synthase, and adenosylcobalamin located within the mitochondria with its cognate enzyme methylmalonyl coenzyme A (CoA) mutase (Gherasim et al., 2013; Watkins and Rosenblatt, 2013). There is the added complication of translocation through the body of multicellular organisms, requiring some form of vascular transport.

Therefore, from their prokaryotic origins, cobamides such as cobalamin undergo a complex journey through many different domains and kingdoms of life, a journey that involves scavenging, recycling, modification, and compartmentalization. In terms of understanding the role played by cobamides in ecology, health, and disease there is a need to devise sensitive methods to follow the nutrient on this biological voyage. Following the movement of cobamides has proved difficult as the nutrient is normally required in small quantities. One way of following cobamides along their transformation and transportation chain is to use fluorescent derivatives coupled to the cobalamin molecule to allow its detection via

fluorescence microscopy (Lee and Grissom, 2009; Smeltzer et al., 2001). The most common of these fluorescent cobalamin derivatives involve attachment of a fluorophore to either the cobalt ion or to the ribose ring of the lower nucleotide. However, attachment to the cobalt ion involves modifications that are usually light sensitive, whereas conjugation to the ribose can be easily removed through nucleotide loop remodeling when such molecules are taken up by bacteria. Attachment of fluorophores to the side chains of the corrin macrocycle have also been reported. However, this attachment requires the hydrolysis of one of the amide side chains and the separation of a range of derivatives prior to the modification. This is low yielding process. Alternatively, a fluorophore could also be attached to the carboxylic acid side chain of cobyric acid, but this would prevent the molecule from being converted into a cobalamin analog *in vivo*. Herein, we describe ways to attach fluorophores directly to the C5 position of the corrin ring according to our understanding of how the corrin ring is constructed. We also report on which of these C5-modified corrin variants, together with some ribose-modified fluorophores, are taken up by a range of different organisms.

RESULTS

Synthesis of C5-allyl-HBA

The transformation of uroporphyrinogen III into a corrin involves, among other events, the addition of 8 S-adenosyl-L-methionine (SAM)-derived methyl groups, the last of which is added to the C5 position (Deery et al., 2012; Warren et al., 2002). We hypothesized that it may be possible to use SAM analogs, with extended chain lengths, to alkylate the C5 position (Figure 2). This requires the isolation of precorrin-7, the substrate for the final methyltransferase, CobL. We recently reported the construction of a recombinant *Escherichia coli* strain from which precorrin-7 can be purified (Deery et al., 2012). Methylation of precorrin-7 by CobL generates precorrin-8, which is isomerized by CobH to generate hydrogenobyrinic acid (HBA). We sought to modify the C5 position by employing an allyl analog of SAM (Dalhoff et al., 2006a, 2006b) with a view to making the respective C5-modified HBA derivative (C5-allyl-HBA) (Figure 2).

When precorrin-7 was incubated with CobL, CobH, and allyl-SAM the color of the solution changed from yellow to orange, consistent with the expected enzymatic transformation. The observed shift in the UV-visible spectrum of the starting material with a maximum absorption at 400 nm to a new species with maxima at 328, 520, and 555 nm is characteristic of the formation of an HBA-like molecule. Analysis of the reaction mixture by high-performance liquid chromatography-mass spectrometry (HPLC-MS) identified a new compound with m/z 907.4 (Figure S1). The observed increase in mass and change in UV-visible spectrum confirms the addition of an allyl group to the macrocycle and indicates that migration of the C11 methyl group to C12 has occurred.

The yield of allyl-HBA obtained from this initial reaction was less than 50%, with the other major product being allyl-precorrin-8. The presence of allyl-precorrin-8 suggested that CobH is the rate-limiting step in this reaction sequence. We considered that the lower activity of CobH could be due to spatial constraints resulting from the larger substrate and, therefore, we decided to make a number of structure-based (Shipman et al., 2001) mutations that would introduce more space into the active site, especially around the region of the

protein where the C5 position of the substrate is found. One of these mutations, T85A, did indeed significantly improve the yield, such that the C5-allyl-HBA was obtained in greater than 85% yield.

The structure of the product was further confirmed as being C5-allyl-HBA by X-ray crystallography. This was achieved by determining the structure of the CobH^{T85A}-C5-allyl-HBA product complex at 1.6 Å resolution (Figure 3; Table S1). The extended alkyl group at the C5 position is clearly seen in the structure. Although the T85A mutation of CobH does increase the size of the active site around the C5 position, the allyl group is still constrained, suggesting that further enhancement could be afforded with more rational engineering. The PDB coordinates are deposited under the code PDB: 5N0G.

We also explored the synthesis of C5-propargyl-HBA using a propargyl SAM derivative (Dalhoff et al., 2006a, 2006b). To achieve this outcome it was necessary to prepare the respective SAM analog *in situ* from Se-propargyl-L-homocysteine using a modified SAM synthetase (I117A mutant of hMAT 2A) as the propargyl-SAM analog is not stable at physiological pH (Wang et al., 2013, 2014). Incubation of precorrin-7 with Se-propargyl-Hcy, Mg-ATP, hMAT 2A I117A, CobL, or CobH^{T85A}, resulted in the same characteristic shift in the UV-visible spectrum associated with the formation of an HBA-like chromophore. Analysis of the purified product by HPLC-MS confirmed the addition of a propargyl group with an observed m/z of 905.4 (Figure S1). This approach demonstrated that a number of C5 derivatives could be made using activated SAM variants. The propargyl-compounds have the advantage of being able to be used with click chemistry approaches for further functionalization.

Conversion of the C5-allyl-HBA to Its Cobyric Acid Form

The conversion of HBA to HBA *a,c*-diamide (HBAD) is mediated by CobB, which amidates the acetic acid side chains attached to the C2 and C7 positions of the corrin framework (Figure 2) (Crouzet et al., 1990). Incubation of CobB with C5-allyl-HBA, in the presence of glutamine and Mg-ATP, resulted in the production of C5-allyl HBAD. The product of the reaction was found to have a shorter retention time on the HPLC column and a 2-mass unit decrease in comparison with the starting material, all of which is consistent with the amidation of the *a* and *c* side chains.

In the aerobic biosynthesis of cobalamin, HBAD undergoes cobalt chelation and adenosylation prior to the completion of the amidation reactions by CobQ (Blanche et al., 1995). However, the light-sensitive nature of the adenosylated intermediate makes this a difficult compound with which to do further modifications. We thus sought a way to bypass the metal-insertion stage of the pathway in order to complete the amidation of HBAD to generate hydrogenobyric acid (Hby), the cobalt-free analog of cobyric acid. This was achieved by using the CobQ from *Allochromatium vinosum*, an organism that was shown to accumulate cobalt-free corrinoids when grown in the absence of cobalt (Koppenhagen et al., 1973). The purified recombinant *A. vinosum* CobQ, in the presence of glutamine and Mg-ATP, did indeed catalyze the amidation of the *b, d, e*, and *g* side chains of HBAD, to generate Hby. Similarly, the enzyme also accepted the C5-allyl-HBAD as a substrate and converted it into C5-allyl Hby (Figure 2), whose structure was confirmed by HPLC-MS (m/z

901) (Figure S1) and 2D heteronuclear nuclear magnetic resonance (NMR) spectroscopy (Figure S2; Table S2).

Transformation of the C5-allyl-HBA Analogs into Cobyric Acid Analogs

The allyl group was modified to a primary amine through a thiolene reaction by reacting the C5-allyl-Hby with cysteamine in the presence of the radical initiator VA-044 (2,2′-azobis[2-(2-imidazolin-2-yl)propane]dihydrochloride) (Figure 2). The reaction product, C5-(2-thiopropane-1-aminoethane [TPEA])-Hby, was confirmed by HPLC-MS (Figure S1). Cobalt was inserted chemically using $CoCl_2$ in dilute aqueous ammonia at elevated temperature. The reaction was quenched with KCN and the product was purified by RP18 chromatography. The structure of the C5-(TPEA)-cobyric acid was confirmed by HPLC-MS (Figure S1) and NMR (Figure S3; Table S2). Together, all of these steps demonstrate how a combination of *in vitro* enzyme-mediated transformations coupled with chemical approaches allow the construction of a regio-specifically derivatized form of cobyric acid (Figure 2).

C5 Fluorophore Attachment

To attach the fluorophores BODIPY TR-X (BoD) and Oregon green 514 (OG) to the terminal amine of the C5 extension, the amine was reacted with the N-hydroxysuccinimide ester of the fluorophore (Figure 2). All of the products were analyzed by HPLC-MS and purified by semi-preparative HPLC. As a result it was possible to generate both BoD and OG C5-linked forms of cobyric acid (Figure 4). These compounds were further characterized in terms of their functionality and uptake in biological systems as described below.

Synthesis of Ribose-Linked Analogs

The ribose-linked analogs were synthesized by carbonyldiimidazole coupling of ethylene diamine to the C5-OH of the ribose moiety of vitamin B_{12}, then the primary amine was linked to the N-hydroxysuccinimide ester of either OG or BoD (Figure 4). These were made following previously published methods for the construction of ribose-linked analogs of cobalamin (Horton et al., 2003; McEwan et al., 1999). The products were analyzed by HPLC-MS, and purified by semi-preparative HPLC. Making both fluorescently labeled cobyric acid and cobalamin derivatives provided the opportunity to compare their respective activities in terms of their ability to be transported into biological systems and ability to act as functionalized nutrients.

Biological Activity of the Corrin Analogs

The biological activity of the C5-cobyric acid analogs as well as the ribose-linked derivatives was investigated initially by comparing their effect in a B_{12}-dependent microbial bioassay (Raux et al., 1996). In this case, an agar plate embedded with B_{12}-dependent reporter strain of *Salmonella enterica* (AR3612; *cysG, metE*) was used to detect growth around an application point, where the size of any resulting growth circle can be measured against growth observed with known amounts of B_{12}. With the microbial bioassay we looked at the efficacy of the C5-(TPEA)-cobyric acid, the BoD, and OG C5-cobyric acid, as well as the BoD and OG ribose analogs of cobalamin, to support growth of the strain. The

observed growth circles can be seen in Figure 5. We were initially surprised to see that the C5-(TPEA)-cobyric acid and the two fluorescently labeled versions of cobyric acid and cobalamin all promoted growth, albeit they needed to be added at much higher concentrations than cyanocobalamin. The requirement for a higher concentration of the analog not only likely reflects poorer molecular recognition by the uptake mechanism but also recognition by methionine synthase. The cobalamin derivatives were more active than the C5 analogs, and the OG derivatives were more active than the corresponding BoD compounds. The reduced efficacy of the cobyric acid analogs in comparison with the cobalamin analogs is probably because the cobyric acid intermediates have to be converted into cobalamin forms before growth can occur.

Uptake of Analogs into Bacteria

We next investigated the uptake of the fluorescent forms of cobyric acid and cobalamin into *E. coli* BL21 (DE3). The BL21 strain has a mutation in *btuB*, which encodes the outer membrane transport component of the cobalamin uptake system (Studier et al., 2009). To overcome this limitation, the BL21 cells were transformed with pLysS-*btuB* and induced overnight with isopropyl β-D-1-thiogalactopyranoside, at which point 1 μM of the OG analogs were added. The bacteria were then imaged by wide-field fluorescence microscopy and the resulting images demonstrated that, while *E. coli* is able to take up both OG fluorescent analogs, significantly greater fluorescence was observed with the cobalamin derivative, suggesting that it is taken up more efficiently.

For the BoD analogs, *E. coli* OP50 cells were transformed with a plasmid harboring both *btuB* and *btuF* (pET-BAD-btuB-btuF), where *btuF* encodes the periplasmic cobalamin binding protein of the B_{12} transporter. These were cloned in order to ensure maximal uptake of the corrin analogs, which were added to a final concentration of 1 μM at the same time as the cells were induced. Cells were incubated separately with C5-BoD-cobyric acid, ribose-BoD-cobalamin, or the unattached BoD fluorophore. As judged by the internal fluorescence of the bacteria, both the C5-BoD and ribose-BoD analogs were seen to accumulate within the cells, indicating that these compounds can be used to monitor transport into *E. coli* (Figure 5). No internal fluorescence was observed with the unattached BoD fluorophore. The significance of using *E. coli* OP50 is that this strain can also be used as a source of food for nematodes such as *C. elegans*.

The BoD analogs of cobalamin were also incubated with *E. coli* BL21 (DE3) and JM109 cells. No fluorescence was observed with the BL21 (DE3) cells, indicating that the defective *btuB* gene prevent uptake of the analog, even at high (1 μM) concentrations. In contrast, uptake of the C5-BoD-cobyric acid analog into JM109 cells was detectable at levels of 10 nM, while the ribose-BoD-cobalamin analogs was detectable at a concentration of 100 nM (Figure S4). These results demonstrate that the uptake of the analogs is dependent upon the presence of a functional BtuB, and that there is some variance between the analogs in regard to molecular recognition by the uptake mechanism.

There is always the possibility that the fluorescently labeled compounds undergo breakdown within the cell. To investigate the possibility of the breakdown of the analogs, we extracted both the ribose-OG-cobalamin and the C5-BoD-cobyric acid analog from *E. coli* that had

been grown in their presence. In both cases we were able to extract the analogs intact from the cells after several days of growth. No evidence for degradation of the compounds was observed (Figure S5).

We also investigated the uptake of the BoD analogs into *Mycobacterium tuberculosis*. Although *M. tuberculosis* has a B_{12} pathway it is missing CobF (Gopinath et al., 2013a, 2013b; Rodionov et al., 2003) and cannot make its own cobalamin. Moreover, *M. tuberculosis* has a different B_{12} uptake mechanism, employing BacA as a transporter (Gopinath et al., 2013a, 2013b). We investigated B_{12} uptake into a B_{12}-dependent strain of *M. tuberculosis*, H37Rv, which carries a mutation in *metE* (H37Rv-metE) (Warner et al., 2007). After growth in Sauton's defined medium, supplemented with either the C5-BoD-cobyric acid or the ribose-BoD-cobalamin, the cells were found to be fluorescent after 24 and 48 hr, respectively, using fluorescence microscopy (Figure 5). It is clear, therefore, that *M. tuberculosis* can take up analogs of both cobyric acid and cobalamin, and that both of these can support growth.

B_{12} Uptake into *C. elegans*

Several recent papers have demonstrated that a free-living nematode, *C. elegans*, represents a good eukaryotic model system to study B_{12} as a nutrient (Bito et al., 2013, 2017; Watson et al., 2014). Like humans, *C. elegans* requires B_{12} for the activities of both B_{12}-dependent methionine synthase and methylmalonyl CoA mutase. Thereby, B_{12} deficiency causes infertility, retarded growth, and reduced lifespan (Bito et al., 2013). Bioinformatic analysis has revealed the presence in the *C. elegans* genome of genetic orthologs associated with human inherited B_{12} disorders but, interestingly, there is no evidence of the main B_{12} binding and trafficking proteins such as intrinsic factor or transcobalamin (Yilmaz and Walhout, 2014). To investigate B_{12} uptake into *C. elegans*, nematodes of the N2 Bristol strain were fed with *E. coli* OP50 that had been grown in the presence of either C5-BoD-cobyric acid, ribose-BoD-cobalamin, or unattached BoD. L4 worms that had been grown in the presence of these analogs since their embryonic stage were imaged on a confocal microscope. Only worms fed on *E. coli* containing the ribose-BoD-cobalamin revealed any fluorescence within the body. Interestingly, confocal microscopy revealed that, in these worms, the fluorescence was localized to discrete spots in the head, vulva, and tail regions, corresponding to the coelomocytes (Figure 6). Even within this discrete cell type, the fluorescence appears to show a degree of sub-cellular localization or compartmentalization (Figure 6). This result demonstrates that *C. elegans* is able to absorb and retain the BoD-labelled cobalamin (which was concentrated in some organs), whereas retention of the C5-cobyric acid analog was clearly absent.

B_{12} Uptake into Higher Plants

It is generally accepted that land plants neither make nor require B_{12} and live in a B_{12}-less world. Early reports suggesting that some plants contained B_{12}-dependent enzyme activity were later put down to bacterial contamination. However, there does appear to be some evidence suggesting that some plants can at least take up and transport cobalamin if the nutrient is cultivated with organic fertilizers or if plants are grown in B_{12}-enriched media (Mozafar, 1994; Sato et al., 2004).

To investigate this observation further, we instigated an outreach project with a local secondary school, where pupils grew *Lepidium sativum* (garden cress) aseptically on an agar medium containing increasing concentrations of vitamin B_{12}. After growth for 7 days the cotyledons from the germinating seedlings were removed, washed, and homogenized. The soluble supernatant after centrifugation was then applied to bioassay plates, which demonstrated that the seedlings were able to absorb cobalamin from the growth medium in a concentration-dependent manner (Figure S6). To confirm the ability of *L. sativum* to absorb cobalamin we repeated the uptake experiment using ribose-OG-cobalamin. *L. sativum* was therefore grown with ribose-OG-cobalamin and, after sectioning, was imaged by confocal microscopy. This approach confirmed that *L. sativum* absorbs ribose-OG-cobalamin, which was found to localize to the vacuoles of the cotyledons (Figure 7). These results provide definitive evidence that some plants can absorb and transport cobalamin, at least by passive diffusion. The linear shape of the concentration response and high amounts of Cbl used in the experiment (see Figure S6) indicate an unspecific uptake mechanism.

DISCUSSION

In this research we have demonstrated that it is possible to functionalize the main corrin framework by substituting the methyl group of SAM with either an allyl or propargyl group. Although this approach was used to modify the C5 position, in theory it may be possible to modify any of the positions on the corrin ring that are methylated by SAM-dependent methyl transferases. Through this development we have shown that it is possible to generate either C5-allyl or C5-propargyl derivatives of HBA, and outlined how these can be transformed into cobyric acid analogs. By attaching fluorophores to the activated C5-allyl group it was possible to make C5-BoD and C5-OG cobyric acid derivatives. This has been achieved through the application of enzymatic and chemical tools to functionalize the comparatively inert corrin framework of B_{12}. In doing so, we have been able to make analogs that can be used to investigate specific biological processes, expanding upon our initial research that allowed us to make different metal isosteres of cobalamin (Widner et al., 2016). Our chemical and biological synthesis approach allows for a regio-specific modification to the corrin molecule. Other have developed methods to generate a reactive group on the corrin molecule through non-specific acid hydrolysis of cobalamin in order to isolate variants with a free acid side chain, which was then subsequently modified (Waibel et al., 2008). This involves elaborate purification procedures and overall low yields.

The success of our approach relies on combining biosynthetic enzymes with chemical synthesis to produce new functional analogs. We wondered whether the additional chemical space occupied around the C5 position would present a steric hindrance, especially with the downstream biosynthetic enzymes. Indeed, the presence of the C5-allyl group on precorrin-8 did reduce the rate of reaction with CobH, which catalyses the methyl migration from C11 to C12 in the formation of HBA. However, with knowledge of the 3D structure of the enzyme (Shipman et al., 2001) we were able to rationally engineer more space into the active site of CobH to make it significantly more active with the C5 analogs.

The amide groups in cobalamin are added by CobB and CobQ. CobB accepts the C5-allyl-modified substrate well and transforms it into C5-HBA *a,c*-diamide in high yields. Normally,

the next steps in the aerobic cobalamin pathway involve metal chelation and adenosylation. The amidation of the remaining side chains is only completed after the chelation and adenosylation processes have taken place. We wanted to change sequence of pathway reactions by completing the amidations prior to metal chelation, i.e., to transform HBAD into Hby. We were aware that some organisms must be able to make Hby as an intermediate, as reports from 40 years ago had highlighted that bacteria such as *A. vinosum*, when grown in the absence of cobalt, are able to produce cobalt-free corrinoids such as hydrogenobalamin (Koppenhagen et al., 1973). We thus cloned *cobQ* from *A. vinosum* and demonstrated that the encoded enzyme is indeed able to convert HBA-diamide into Hby and similarly convert the C5 analogs into the C5-Hby equivalents. With all these enzyme tools in hand we were able to produce the C5-allyl Hby on the tens of mg scale. After coupling of the fluorophore to the C5-allyl position cobalt was then inserted to generate the C5-cobyric acid analogs containing either an OG or BoD fluorophore. These cobyric acid analogs were then compared with cobalamin analogs where the fluorophores were attached to the ribose position.

The functional analysis of the various corrin and cobalamin analogs was surprising. Addition of the C5-(TPEA)-cobyric acid to a microbial B_{12} bioassay plate promoted growth around the application point, indicating that the C5 material must be taken up by the *S. enterica* reporter strain, which then presumably converted it into a functional cobalamin analog. The other analogs such as the C5-OG and C5-BoD variants also promoted growth, albeit less well. The high levels of the analogs required to promote growth reflect several constraints on their molecular recognition in terms of their uptake and incorporation into methionine synthase. For instance, it is clear from our results that the ribose-OG-cobalamin is taken up more efficiently than the C5-linked cobyric acid analog, while, conversely, the C5-BoD-cobyric acid analog is taken up more easily that the ribose-linked cobalamin equivalent. What is most surprising of all is that all these analogs appear to fit into the active site of methionine synthase. The crystal structure of the *E. coli* methionine synthase suggests that there is a certain amount of room to accommodate some extra bulk on the ribose group (Drennan et al., 1994). However, within the corrin binding site there is less room for the further chemical space required for the C5 attachment. Nonetheless, as mentioned above, the same is true with CobH, the enzyme required to convert the modified C5-allyl-precorrin-8 intermediate into C5-allyl-HBA, where the enzyme still catalyses the reaction, albeit at a reduced rate in comparison with the natural substrate. So, with methionine synthase the extra group on the corrin ring may force some conformational change within the protein so that the extra bulk is accommodated. There is always the possibility that the fluorescent analogs are broken down in the cell to release the fluorophore from the corrin. However, extraction of C5-BoD-cobyric acid from *E. coli* that had been grown with the compound resulted only in the identification of intact C5-BoD-cobyric acid. Overall, this tells us that the *S. enterica* and *E. coli* uptake mechanisms will accept corrin and B_{12} analogs with significant extra chemical bulk and that these compounds are relatively active inside the cell.

We investigated whether these fluorescent corrin analogs were also taken up by *M. tuberculosis*. Interestingly, both the C5-BoD-cobyric acid and the ribose-BoD-cobalamin analogs were taken up by cultured *M. tuberculosis* cells, with the C5-BoD analog appearing to be taken up more quickly than the ribose analog. Significantly, both analogs appear to

support growth of this B_{12}-dependent tuberculosis (TB) strain indicating that the molecules are able to get inside the cells. The B_{12} uptake mechanism in *M. tuberculosis*, which is different to that found in most other bacteria (Gopinath et al., 2013a, 2013b), is clearly able to take up incomplete corrinoids. As humans are not able to take up cobyric acid, the use of cobyric acid conjugates could prove a useful method for specifically labeling and targeting TB infections.

There is still much to learn about how B_{12} makes its journey from bacteria to specific compartments in eukaryotic cells. Several recent reports have highlighted the fact that *C. elegans* may prove to be a good model to learn more about the movement, distribution, and storage of B_{12} (Bito et al., 2013, 2017; Watson et al., 2014; Yilmaz and Walhout, 2014). Indeed, we were able to show that a fluorescent B_{12} derivative is absorbed from bacteria by *C. elegans* and is observed to accumulate within coelomocytes. Interestingly, only the ribose-linked cobalamin analog was absorbed indicating that the worm is able to differentiate between complete and incomplete corrinoids. It is not clear whether this is due to the B_{12} analog being recognized as foreign material or whether the cells represent a storage area for excess cobalamin. Nonetheless, the results demonstrate that this is a powerful model to learn about how B_{12} is absorbed and, as this system is different to mammalian systems, there is the possibility of exploiting this difference to try and treat worm-based parasite such as hook worms.

It is well documented that vegetarians are more prone to B_{12} deficiency as plants lack B_{12} (Stabler and Allen, 2004). However, it has been suggested that some plants are able to absorb the nutrient if added exogenously to their growth media (Mozafar, 1994; Sato et al., 2004). Through an outreach project we demonstrated that that garden cress, *L. sativum*, can indeed take up cobalamin. The amount of B_{12} absorbed by garden cress is dependent upon the amount present in the growth medium, and displayed a linear rather than a hyperbolic relationship. This would suggest an unspecific form of uptake. Nonetheless, we were able to confirm B_{12} uptake using our OG analog of cobalamin, showing that the nutrient ends up in the vacuole in the leaf. The uptake of B_{12} into plants is irrelevant in terms of plant metabolism, since plants do not possess any B_{12}-dependent enzymes, but the finding that some plants are able to accumulate B_{12} is important, as such nutrient-enriched plants would be important in helping overcome dietary limitations in countries such as India, which have a high proportion of vegetarians.

STAR★METHODS

CONTACT FOR REAGENT AND RESOURCES SHARING

Further information and requests for resources and reagents should be directed to and will be fulfilled by the Lead Contact, Professor Martin J. Warren (m.j.warren@kent.ac.uk)

EXPERIMENTAL MODEL AND SUBJECT DETAILS

All bacterial strains used in this study are listed in the Key Resources Table together with their source and genotypes. For *E. coli*, unless stated otherwise, the strains were grown in LB media supplemented with the appropriate antibiotics. All *Mycobacterium tuberculosis*

cultures were grown in cobalamin deficient Sauton's defined medium (0.5 g KH_2PO_4, 0.5 g $MgSO_4 \cdot 7H_2O$, 2 g citric acid, 0/05 g ferric ammonium citrate, 60 mLs glycerol, 4 g asparagine and 500 μL TWEEN 80 in 1 L pH 7.0. Worm studies were carried out with *Caenorhabditis elegans* var. Bristol (strain N2) and maintained on nematode growth medium (NGM) agar.

METHODS DETAILS

Chemicals and Reagents—Oregon Green® 514 (OG) and BODIPY® TR-X (BoD) succinimidyl ester were both purchased from Thermo Fisher Scientific, Inc., as was the P-Per for plant extraction. Allyl-Bromide, Cysteamine hydrochloride, Seleno-L-methionine, Dowex 50WX4 hydrogen form, Diethylaminoethyl-Sephacel, and N, N-DiisopropylethylamineReagentPlus® were bought from Sigma Aldrich, Ltd. Other chemicals and equipment include LICHROPREP RP-18 from VWR, VA-044 2,2'-Azobis[2-(2-imidazolin-2-yl)propane] dihydrochloride from alpha laboratories Ltd. and crystal screens from Molecular Dimensions Ltd.

Protein Production and Purification—All cobalamin biosynthetic genes were amplified by PCR using genomic DNA from either *Rhodobacter capsulatus* SB1003 (*cobL, H* and *B*), or *Allochromatium vinosum* ATCC 17899 (*cobQ*). The cob genes were amplified individually with primers then cloned into modified pET14b plasmids. These were then transformed into BL21 star (DE3) pLysS. hMATIIA I117A was transformed into Rosetta 2 (DE3) pLysS. The recombinant strains were grown in LB at 37°C and protein overexpression was induced with 0.4 mM of isopropyl-1-thio-β-D-galactopyranoside. The cells were resuspended in buffer A (20 mM Tris pH 8, 500 mM NaCl, 10 mM Imidazole) and sonicated. The protein was purified using Chelating Sepharose™ charged with $NiSO_4$. Unbound proteins were washed off with buffer A, buffer A containing 30 mM imidazole and buffer A containing 80 mM Imidazole. Proteins were eluted with buffer A containing 400 mM imidazole and passed through a PD10 column equilibrated with buffer B (20 mM Tris, pH 8.0, containing 100 mM NaCl) for CobL and H, or buffer C (20 mM Tris, pH 8.0, containing 500 mM NaCl) for CobB and Q.

Production and Purification of Precorrin-7—*E. coli* BL21 star (DE3) pLysS was transformed with pET3a/cobA-I-G-J-M-F-K-L^C-E and grown in 2TY at 28°C for 24 hours (Deery et al., 2012). The cells were resuspended in 20 mM Tris, pH 8.0, and sonicated. Proteins were precipitated with acetonitrile and following clarification by centrifugation precorrin-7 was purified over DEAE-Sepherose. The column was washed with 20 mM Tris, pH 8.0, containing 100 mM NaCl, before elution with 500 mM NaCl. The pH of the eluent was lowered to pH 4.0 with TFA and the precorrin-7 was further purified over RP18. The column was washed with a stepwise gradient of methanol in 0.1% (v/v) TFA and elution was achieved with 50% methanol.

Synthesis of SAM Analogues—Allyl-SAM was prepared from homocysteine and allylbromide as described previously (Wang et al., 2011). Allyl bromide (44 μL, 0.214 mmol) and $AgClO_4$ (6 mg, 0.025 mmol) were added to S-adenosyl-*L*-homocysteine (5 mg, 0.013 mmol) dissolved in a mixture of formic acid and acetic acid (1:1, 0.6 mL) at 0°C. The

mixture was allowed to warm up to room temperature and stirred continuously for 2.5 h. A further portion of allyl bromide (44 μL, 0.214 mmol) and $AgClO_4$ (6 mg, 0.025 mmol) were added and the reaction mixture was stirred for another 2.5 h. following centrifugation to remove the precipitate, H_2O (3 mL) was added and the residual allyl bromide was extracted with diethyl ether (5 mL × 3). The aqueous phase was then concentrated under vacuum.

Synthesis of Se-propargyl-L-selenohomocysteine—Se-propargyl-L-selenohomocysteine was synthesized from L-selenomethionine as described previously (Singh et al., 2014). L-selenomethionine (100 mg) was dissolved in 20 mL liquid ammonia at −78°C and stirred. Small fragments of sodium metal (34 mg) were added until a deep blue colour persisted for at least 1 min. Progargyl bromide (46.5 μL) was then added followed by ammonium chloride (20 mg). The reaction removed from the cooling bath and the flask was left open to the atmosphere for the ammonia to evaporate. The resulting residue was dissolved in H_2O (5 mL) and the pH was adjusted to pH 5 - 7 by the addition of HCl (1 M). The solvent was removed under reduced pressure.

Synthesis C5-allyl-HBA—Precorrin-7 (60 μM) was incubated with CobL(6 μM), CobH (30 μM) and allyl-SAM (170 μM) in buffer Bat 28°C for 16 hours in the dark. The reaction mixture was then heated to 65°C and the precipitate was removed by centrifugation. The resulting supernatant was applied to a DEAE-Sepharose column equilibrated in 20 mM Tris, pH 8.0. The column was washed with 20 mM Tris, pH 8.0, and the product was eluted with 20 mM Tris, pH 8.0, containing 500 mM NaCl.

Synthesis of C5-propargyl-HBA—C5-propargyl-HBA was prepared from precorrin-7 and Se-propargyl-L-selenohomocysteine. Precorrin-7 (60 μM), Se-propargyl-L-selenohomocysteine (1.5 mM), ATP (2 mM), $MgCl_2$ (5 mM), hMAT2A I117A (60 μM), CobL (6 μM), CobH (30 μM), Se-propargyl-Hcy (1.5 mM) and SAHH (50 μM) were incubated in 20 mM Tris, pH 8.0, containing 100 mM NaCl at 28°C in the dark for 16 h. The reaction mixture was heated to 80°C for 15 minutes and the precipitate was removed by centrifugation. The supernatant was applied to DEAE column pre-equilibrated in 20 mM Tris, pH 8.0. The column was washed with 20 mM Tris, pH 8.0, containing 100 mM NaCl, and eluted with 20 mM Tris, pH 8.0, containing 500 mM NaCl.

Synthesis of C5-allyl-Hby—C5-allyl-HBA (30 μM), CobB (2 μM), CobQ (5 mM), ATP (8 mM), L-Glutamine (8 mM), and $MgCl_2$ (20 mM) were incubated in buffer C at 28°C for 16 hours in the dark. The reaction mixture was heated to 80°C, acidified to pH 4 with trifluoroacetic acid (TFA) and the precipitate removed by centrifugation. The supernatant was applied to an RP18 column equilibrated in 0.1% TFA, washed with 0.1% TFA followed by 20% methanol before elution in 50% methanol. The product was then dried in a vacuum centrifuge.

C5 Allyl Group Extension—The C5-allyl group was modified through a thiol-ene coupling reaction with cysteamine. A solution of C5-allyl-Hby (30 μM) was incubated at 55°C in acetate buffer (pH 4.0, 0.25 M) containing cysteamine (100 mM) and VA-044 (20 mM) in the dark for 15 mins. The product was purified over RP18 and analyzed by HPLC-MS.

Cobalt Insertion—Cobalt insertion was achieved through incubation of the desired metal-free corrinoid (20 μM) with $CoCl_2$ (10 mM) in ammonium hydroxide (0.2 M) at 80°C under an N_2 atmosphere. The reaction was followed UV-visible spectroscopy until deemed complete (~ 60 mins) after which it was quenched with KCN and the product purified over RP18 and eluted in methanol.

Synthesis of Fluorescent C5-Cobyric Acid Derivatives—CN_2-C5-TPEA-cobyric acid was dissolved in DMSO and either the succinimidyl ester of OG or BoD along with 2 equivalents of DIPEA were added. The reaction was stirred at room temperature for 16 hours in the dark. The solvent was removed *in vacuo* and the compound was purified by semi-preparative HPLC.

Ribose Linked Fluorescent Vitamin B_{12} Derivatives—The ribose-5'-hydroxyl group of vitamin B_{12} was activated with carbonyldiimidazole and coupled with 1,2-diaminoethane as described previously (McEwan et al., 1999). The derivative was added to either the succinimidyl ester of OG or BoD with 2 equivalents of DIPEA in DMSO. The reaction was stirred for 16 hours in the dark at room temperature. The product was precipitated with acetone and collected by filtration. Fluorescent derivatives were dissolved in 50% acetonitrile and purified by semi-preparative HPLC.

Crystal Structure Determination of $CobH^{T85A}$ with Bound C5-allyl-HBA—Recombinantly produced $CobH^{T85A}$ was purified on a nickel affinity column. After affinity purification $CobH^{T85A}$ was subject to gel filtration on a G200 Superdex column (GE Healthcare). Protein fractions were collected and concentrated to 7 mg mL^{-1}. Allyl-HBA was added to the protein in a 1:1 ratio prior to crystallisation at 19°C using the hanging drop vapour diffusion method. Initial crystals were obtained in 0.2 M calcium acetate hydrate, 0.1 M sodium cacodylate pH 6.5,18 % (w/v) PEG 8000 (Molecular Dimensions, MD01 condition 20). Crystal optimisation required the addition of 20% methanol to the well condition and increasing the PEG 8000 to 20%. This resulted in multiple square shaped crystals which formed within three days. A single crystal was picked, transferred to a drop of in 0.2 M calcium acetate hydrate, 0.1 M sodium cacodylate pH 6.5, 20 % (w/v) PEG 8000 containing 20% glycerol as a cryoprotectant and then flash frozen in liquid nitrogen. The crystal diffracted to 1.6 Å and was found to belong to space group C 1 2 1 which is the same as the published structure of *R. capsulatus* CobH co-crystallised with HBA (PDB 4AU1) (Deery et al., 2012). Data for the crystal was collected using beamline IO4–1 at the Diamond Light Source (UK). The data was auto-integrated and scaled using the Xia2 package using XDS (X-ray data software) and XSCALE (3dii) at the beamline. An initial model was generated by refinement of the scaled and merged data against PDB:4AU1 in Refmac 5. The model was then refined through cycles of manual model building in Coot and refinement with Refmac 5. The final model was validated in Coot and with wwPDB. The PDB coordinates were deposited with the code 5N0G.

Bioassay Plates—A quantitative bioassay using *S. typhimurium* AR3612 was performed as described previously (Rauxet al., 1996). The bioassay plates containing the indicator strain AR3612 were prepared from lawns of the corresponding bacteria. The bacteria were

scraped from an overnight minimal medium (M9) plate containing methionine (50 mg/L) and cysteine (50 mg/L) and washed with 0.9 % (w/v) NaCl to remove traces of methionine. The cells were mixed with 300 mL of minimal medium (M9) containing cysteine (50 mg/L) agar at 47°C, and poured into plates.

Imaging in *Escherichia coli*—TheOP50 *E. coli* was transformed with pET-BAD-btuSFand grown in a 4 mL LB culture after inoculation with 16 μL of starter culture. This was grown with 1 μM of C5-BoD-cobyric acid or ribose-BoD-cobalamin overnight with induction with 0.02% arabinose. Cultures (1 mL) were spun down and washed three times with fresh LB to remove external fluorophore. The final pellet was resuspended in 1 mL of fresh LB, 5 μL of this culture was dried on to a 1 % (w/v) LB-agarose pad and imaged on an Olympus IX81 widefield microscope with PlanApo 150 × OTIRFM-SP 1.49 numerical aperture lens mounted on ASI stage (Applied Scientific), and illuminated using LED light sources (Cairn Research Ltd) with appropriate filters (YFP and mCherry, Chroma). The samples were visualised using a Princeton ProEM 1024 back-thinned EMCCD camera (Princeton Instruments) on Metamorph software (Molecular Devices). Each 3D-maximum projection of volume data was calculated from 13 *z*-plane images, each 0.2 μm apart.

Imaging in *Mycobacterium tuberculosis*—Relevant strains of *M. tuberculosis* were grown in 150 μL cultures in a 96 well plate containing various concentrations of the BODIPY-labelled analogues of cobalamin and cobyric acid. The cells were grown for up to 48 h. After growth, the cells were spun down and washed three times to remove the fluorophore. Cells were pipetted directly onto a slide and imaged live on a Leica SP5 microscope using 594 nm excitation and imaging between 600-700 nm. The images were processed using Leica Lite confocal software and FIJI (Schindelin et al., 2012).

Extraction of Cobalamin from *Lepidium sativum* Using P-Per—*Lepidium sativum* seeds were sterilised by washing with 70 % ethanol three times then rinsed five times with sterile water. The seeds were placed on Murashige-Skoog agar containing different concentrations of cobalamin, and grown for one week in sunlight at room temperature. The cotyledons of the cress were collected and washed 5 times with water. The residual water was removed by pipette, after centrifugation. The P-Per was prepared as instructed in the enclosed manual (Thermo Fisher): 283 μL reagent A, 2.9 μL of reagent B, and 214 μL of reagent C. A little sand was added to the cotyledons along with 100 μL of the P-Per. The cotyledons were ground using a hand-held pellet pestle for 2 minutes. The suspension was vortexed and then centrifuged for 3 minutes at 15,000 rpm rotation. The lower aqueous phase was collected and applied to the bioassay plate as described above.

Imaging in *L. sativum*—*L. sativum* seeds were sterilised by washing with 70 % ethanol three times, then rinsed five times with sterile water. The seeds were placed on the Murashige-Skoog agar with 0.5 μM ribose-OG cobalamin, and grown at room temperature in the dark for five days. Whole cotyledons or sectioned cress were placed directly on the glass slide with water. The samples were imaged with a Leica TCS SP2 laser scanning confocal microscope (Leica Microsystems, Germany) with AOBS (Acoust-Optical Beam Splitter) detected using PMTs (photomultiplier tubes). Both the 40 × and 63 × HCX PL

APO oil lenses, numerical aperture 1.25 and 1.4 respectively, were used. Samples were excited at 514 nm from an Argon–Krypton-mixed gas laser and images were acquired in the green/yellow region of the light spectrum (525–590 nm). The software used to image was LCS (Leica Confocal Software) and the images were processed using Leica Lite confocal software and FIJI (Schindelin et al., 2012).

Imaging in *Caenorhabditis elegans*—*C. elegans* were maintained on normal *E. coli* OP50 at 20°C unless otherwise stated. A food source carrying the fluorescent analogues was made by transforming the OP50 with pET-BAD-*btuSF* and were grown in a 4 mL LB culture after inoculation with 16 μL of starter culture. This was incubated with 1 μM of C5-BoD-cobyric acid or ribose-BoD-cobalamin overnight with induction with 0.02% arabinose. 1 mL of culture was spun down and washed three times with fresh LB to remove external fluorophore. The final pellet was resuspended in 1 mL of fresh LB and 200 μL of the OP50 culture was pipetted on to the centre of NGM agar plates. These plates were left to dry in a sterile culture hood for 4 hours and then stored at 4°C until used. Three forth larval stage (L4) *C. elegans* were transferred to the seeded plates and left to grow at 20°C for four days before imaging. Three third larval stage (L3) *C. elegans* were transferred to the seeded plates and allowed to lay eggs. These progeny were then imaged at the L4 stage.

For each slide, 3-5 L4 stage *C. elegans* were mounted in M9 + 0.2 % levamisole on a 2 % agarose pad and imaged within 30 min at the University of Bristol on a Leica SP8X AOBS confocal laser scanning microscope attached to a Leica DMi8 inverted epifluorescence microscope with ‘Adaptive Focus Control’. The sample was excited with a white light laser at 594 nm and detected between 599-712 nm using a hybrid gated detector for the fluorophore, and excited with a 405 nm laser, with images acquired between 410-505 nm for the gut granule autofluorescence. All images were taken using a 20 × numerical aperture 0.75 dry lens. Again the images were processed using Leica Lite confocal software and FIJI (Schindelin et al., 2012).

HPLC MS Analysis—Samples were separated on an Agilent 1000 series HPLC coupled to a micrOTOF-Q II (Bruker) mass spectrometer using an Ace 5 AQ column (2.1 × 150 mm; Advanced Chromatography Technologies) maintained at 30°C and with a flow rate of 0.2 mL/min. The mobile phase consisted of 0.1% TFA (v/v) in water (solvent A) and 100% acetonitrile (solvent B). Three different HPLC gradients were employed. *Gradient 1* (methionine and SAM and analogues): Linear gradient from 0-30% solvent B over 30 mins. *Gradient 2* (pathway intermediates): 5-20% B over 6 mins, 20-30% B over 19 mins followed by 30-90% B over 5 mins. *Gradient 3* (fluorescent cobalamin analogues): Linear gradient from 0-100% solvent B over 45 mins. Semi-preparative HPLC was performed on an Agilent 1000 series HPLC using a CS SIL C18 column (250 mm × 10 mm; 5 μm; Charlton Scientific) at a flow rate of 5 mL/min running the gradients described above.

NMR Analysis—NMR experiments were performed using a 600 MHz (^{1}H) Bruker Avance III spectrometer with a 5 mm QCI-F cryoprobe. Assignments were completed using DQF-COSY, TOCSY (20 ms and 80 ms mixing times), NOESY (500 ms mixing time), ^{13}C-HSQC-TOCSY, ^{13}C,^{1}H-HSQC and ^{13}C,^{1}H-HMBC experiments with WaterGATE or excitation sculpting water suppression on 0.1-1 mM samples dissolved in deuterium oxide.

All ^{13}C data was obtained using natural isotopic abundance. Data were processed and analysed using Bruker Topspin version 3.2 and CCPN analysis. ^{1}H Chemical shift referencing was based on the position of the water resonance, ^{13}C referencing used $^{1}H/^{13}C$ gyromagnetic ratios to define indirect carrier position (Wishart and Case, 2001) and all data were obtained at 25°C.

QUANTIFICATION AND STATISTICAL ANALYSIS

Bioassays (Figures 5 and S6) were performed three times (n=3) and the values for the amount of B_{12} present in the samples was generated from a standard curve. For B_{12} uptake into plants the averages of the separate measurements were then calculated and plotted using Microsoft Excel. The structure of CobH was refined with internal statistical analysis as reported in the deposition in the PDB

No additional statistical tests were performed.

DATA AND SOFTWARE AVAILABILITY

All software used in this study is reported in Method Details and indicated in the Key Resources Table. The coordinates for the CobH T85A crystal structure were deposited in the Protein Data Bank PDB:5N0G (https://www.rcsb.org/structure/5n0g).

Supplementary Material

Refer to Web version on PubMed Central for supplementary material.

ACKNOWLEDGMENTS

This work was supported, in part, by the Intramural Research Program of NIAID and in part by grants from the Biotechnology and Biological Sciences Research Council (BBSRC; BB/L010208/1, BB/K009249/1, and BB/I012079, and the Wellcone Trust 097627/Z/11/Z). We thank Prof Jason Micklefield (Manchester) and Prof Udo Oppermann (Oxford) for the gift of SAHH and hMATIIA. Our research into B_{12} uptake into plants was done as part of an outreach program to engage pupils in real scientific research, inspired by the Authentic Biology project (www.authentic-biology.org). The detection and measurement of B_{12} in the cotyledons of garden cress was performed with the help of the biology teachers and year 11 and 12 pupils at Sir Roger Manwood School in Sandwich, Kent. Teachers: Dr Jackie Wilson and Vicki Beale. Pupils: Megan Battenfield, Megan Betts, Alex Gallagher, Inga Loo, Shiree Kinder, George Morris, Emma Rudge, James Russell, Rebekah Smith, Maddy Stock, Pema Tamang, Elizabeth Westbrook, Himmy Wu, and Katie Fidock.

REFERENCES

Allen RH, and Stabler SP (2008). Identification and quantitation of cobalamin and cobalamin analogues in human feces. Am. J. Clin. Nutr 87, 1324–1335. [PubMed: 18469256]

Banerjee R, and Ragsdale SW (2003). The many faces of vitamin B12: catalysis by cobalamin-dependent enzymes. Annu. Rev. Biochem 72, 209–247. [PubMed: 14527323]

Bito T, Matsunaga Y, Yabuta Y, Kawano T, and Watanabe F (2013). Vitamin B_{12} deficiency in *Caenorhabditis elegans* results in loss of fertility, extended life cycle, and reduced lifespan. FEBS Open Bio 3, 112–117.

Bito T, Misaki T, Yabuta Y, Ishikawa T, Kawano T, and Watanabe F (2017). Vitamin B_{12} deficiency results in severe oxidative stress, leading to memory retention impairment in *Caenorhabditis elegans*. Redox Biol. 11, 21–29. [PubMed: 27840283]

Blanche F, Cameron B, Crouzet J, Debussche L, Thibaut D, Vuilhorgne M, Leeper FJ, and Battersby AR (1995). Vitamin B_{12} - how the problem of its biosynthesis was solved. Angew. Chem. Int. Ed 34, 383–411.

Brito A, Chiquette J, Stabler SP, Allen RH, and Girard CL (2015). Supplementing lactating dairy cows with a vitamin B_{12} precursor, 5,6-dimethylbenzimidazole, increases the apparent ruminal synthesis of vitamin B_{12}. Animal 9, 67–75. [PubMed: 25171056]

Chan CH, and Escalante-Semerena JC (2011). ArsAB, a novel enzyme from *Sporomusa ovata* activates phenolic bases for adenosylcobamide biosynthesis. Mol. Microbiol 81, 952–967. [PubMed: 21696461]

Croft MT, Lawrence AD, Raux-Deery E, Warren MJ, and Smith AG (2005). Algae acquire vitamin B_{12} through a symbiotic relationship with bacteria. Nature 438, 90–93. [PubMed: 16267554]

Crofts TS, Seth EC, Hazra AB, and Taga ME (2013). Cobamide structure depends on both lower ligand availability and CobT substrate specificity. Chem. Biol 20,1265–1274. [PubMed: 24055007]

Crouzet J, Cauchois L, Blanche F, Debussche L, Thibaut D, Rouyez MC, Rigault S, Mayaux JF, and Cameron B (1990). Nucleotide sequence of a *Pseudomonas denitrificans* 5.4 kilobase DNA fragment containing 5 *cob* genes and identification of structural genes encoding *S-adenosyl-L*-methionine - uroporphyrinogen III methyltransferase and cobyrinic acid *a,c*-diamide synthase. J. Bacteriol. 172, 5968–5979. [PubMed: 2211520]

Dalhoff C, Lukinavicius G, Klimasauskas S, and Weinhold E (2006a). Direct transfer of extended groups from synthetic cofactors by DNA methyltransferases. Nat. Chem. Biol 2, 31–32. [PubMed: 16408089]

Dalhoff C, Lukinavicius G, Klimasauskas S, and Weinhold E (2006b). Synthesis of S-adenosyl-L-methionine analogs and their use for sequence-specific transalkylation of DNA by methyltransferases. Nat. Protoc 1, 1879–1886. [PubMed: 17487172]

Deery E, Schroeder S, Lawrence AD, Taylor SL, Seyedarabi A, Waterman J, Wilson KS, Brown D, Geeves MA, Howard MJ, et al. (2012). An enzyme-trap approach allows isolation of intermediates in cobalamin biosynthesis. Nat. Chem. Biol 8, 933–940. [PubMed: 23042036]

Degnan PH, Taga ME, and Goodman AL (2014). Vitamin B_{12} as a modulator of gut microbial ecology. Cell Metab 20, 769–778. [PubMed: 25440056]

Drennan CL, Huang S, Drummond JT, Matthews RG, and Ludwig ML (1994). How a protein binds B_{12} - a 3.0-Angstrom X-ray structure of B_{12}-binding domains of methionine synthase. Science 266, 1669–1674. [PubMed: 7992050]

Emsley P, Lohkamp B, Scott WG, and Cowtan K (2010). Features and development of Coot. Acta Crystallogr. D Biol. Crystallogr 66, 486–501. [PubMed: 20383002]

Gherasim C, Lofgren M, and Banerjee R (2013). Navigating the B_{12} road: assimilation, delivery, and disorders of cobalamin. J. Biol. Chem 288, 13186–13193. [PubMed: 23539619]

Girard CL, Berthiaume R, Stabler SP, and Allen RH (2009). Identification of cobalamin and cobalamin analogues along the gastrointestinal tract of dairy cows. Arch. Anim. Nutr 63, 379–388. [PubMed: 26967796]

Gopinath K, Moosa A, Mizrahi V, and Warner DF (2013a). Vitamin B_{12} metabolism in *Mycobacterium tuberculosis*. Future Microbiol 8, 1405–1418 [PubMed: 24199800]

Gopinath K, Venclovas C, loerger TR, Sacchettini JC, McKinney JD, Mizrahi V, and Warner DF (2013b). A vitamin B_{12} transporter in *Mycobacterium tuberculosis*. Open Biol. 3, 120175. [PubMed: 23407640]

Gray MJ, and Escalante-Semerena JC (2009). *In vivo* analysis of cobinamide salvaging in *Rhodobacter sphaeroides* strain 2.4.1. J. Bacteriol 191, 3842–3851. [PubMed: 19376876]

Greibe E, Fedosov S, and Nexo E (2012).The cobalamin-binding protein in zebrafish is an intermediate between the three cobalamin-binding proteins in human. PLoS One 7, e35660. [PubMed: 22532867]

Helliwell KE, Lawrence AD, Holzer A, Kudahl UJ, Sasso S, Krautler B, Scanlan DJ, Warren MJ, and Smith AG (2016). Cyanobacteria and eukaryotic algae use different chemical variants of vitamin B_{12}. Curr. Biol 26, 999–1008. [PubMed: 27040778]

Horton RA, Bagnato JD, and Grissom CB (2003). Structural determination of 5'-OH alpha-ribofuranoside modified cobalamins via 13C and DEPT NMR. J. Org. Chem 68, 7108–7111. [PubMed: 12946160]

Koppenhagen VB, Wagner F, and Pfiffner JJ (1973). Alpha-(5,6 dimethylbenzimidazolyl)rhodibamide and rhodibinamide, the rhodium analogues of vitamin B_{12} and cobinamide. J. Biol. Chem 248, 7999–8002. [PubMed: 4752943]

Krautler B, Fieber W, Ostermann S, Fasching M, Ongania KH, Gruber K, Kratky C, and Mikl C (2003). The cofactor of tetrachloroethene reductive dehalogenase of *Dehalospirillum multivorans* is norpseudo B_{12}, a new type of a natural corrinoid. Helv. Chim. Acta 86, 3698–3716.

Lee M, and Grissom CB (2009). Design, synthesis, and characterization of fluorescent cobalamin analogues with high quantum efficiencies. Org. Lett 11, 2499–2502. [PubMed: 19441855]

Maggio-Hall LA, and Escalante-Semerena JC (2003). Alpha-5,6-dimethyl-benzimidazole adenine dinucleotide (alpha-DAD), a putative new intermediate of coenzyme B_{12} biosynthesis in *Salmonella typhimurium*. Microbiology 149, 983–990. [PubMed: 12686640]

Martens JH, Barg H, Warren MJ, and Jahn D (2002). Microbial production of vitamin B_{12}. Appl. Microbiol. Biotechnol 58, 275–285. [PubMed: 11935176]

McEwan JF, Veitch HS, and Russell-Jones GJ (1999). Synthesis and biological activity of ribose-5'-carbamate derivatives of vitamin B_{12}. Bioconjug. Chem 10, 1131–1136. [PubMed: 10563784]

Moore SJ, Lawrence AD, Biedendieck R, Deery E, Frank S, Howard MJ, Rigby SE, and Warren MJ (2013). Elucidation of the anaerobic pathway for the corrin component of cobalamin (vitamin B_{12}). Proc. Natl. Acad. Sci. USA 110, 14906–14911. [PubMed: 23922391]

Mozafar A (1994). Enrichment of some B-vitamins in plants with application of organic fertilizers. Plant Soil 167, 305–311.

Potterton E, Briggs P, Turkenburg M, and Dodson E (2003). A graphical user interface to the *CCP*4 program suite. Acta Crystallogr. D Biol. Crystallogr D59, 1131–1137.

Raux E, Lanois A, Levillayer F, Warren MJ, Brody E, Rambach A, and Thermes C (1996). *Salmonella typhimurium* cobalamin (vitamin B_{12}) biosynthetic genes: functional studies in *S. typhimurium* and *Escherichia coli*. J. Bacteriol 178, 753–767. [PubMed: 8550510]

Renz P (1999). Biosynthesis of the 5,6-dimethylbenzidazole moiety of cobalamin and of the other bases found in natural corrinoids In Chemistry and Biochemistry of B_{12}, Banerjee R, ed. (John Wiley and sons), pp. 557–575.

Rodionov DA, Vitreschak AG, Mironov AA, and Gelfand MS (2003). Comparative genomics of the vitamin B_{12} metabolism and regulation in prokaryotes. J. Biol. Chem 278, 41148–41159. [PubMed: 12869542]

Roth JR, Lawrence JG, and Bobik TA (1996). Cobalamin (coenzyme B12): synthesis and biological significance. Annu. Rev. Microbiol 50,137–181. [PubMed: 8905078]

Sato K, Kudo Y, and Muramatsu K (2004). Incorporation of a high level of vitamin B_{12} into a vegetable, kaiware daikon (Japanese radish sprout), by the absorption from its seeds. Biochim. Biophys. Acta 1672, 135–137. [PubMed: 15182932]

Schindelin J, Arganda-Carreras I, Frise E, Kaynig V, Longair M, Pietzsch T, Preibisch S, Rueden C, Saalfeld S, Schmid B, et al. (2012). FIJI: an open-source platform for biological-image analysis. Nat. Methods 9,676–682. [PubMed: 22743772]

Shipman LW, Li D, Roessner CA, Scott AI, and Sacchettini JC (2001). Crystal stucture of precorrin-8x methyl mutase. Structure 9, 587–596. [PubMed: 11470433]

Singh S, Zhang J, Huber TD, Sunkara M, Hurley K, Goff RD, Wang G, Zhang W, Liu C, Rohr J, et al. (2014). Facile chemoenzymatic strategies for the synthesis and utilization of S-adenosyl-(L)-methionine analogues. Angew. Chem. Int. Ed 53, 3965–3969.

Smeltzer CC, Cannon MJ, Pinson PR, Munger JD, Jr., West FG, and Grissom CB (2001). Synthesis and characterization of fluorescent cobalamin (CobalaFluor) derivatives for imaging. Org. Lett 3, 799–801. [PubMed: 11263885]

Stabler SP, and Allen RH (2004). Vitamin B_{12} deficiency as a worldwide problem. Annu. Rev. Nutr. 24, 299–326. [PubMed: 15189123]

Studier FW, Daegelen P, Lenski RE, Maslov S, and Kim JF (2009). Understanding the differences between genome sequences of *Escherichia coli* B strains REL606 and BL21(DE3) and comparison of the *E. coli* B and K12 genomes. J. Mol. Biol 394, 653–680. [PubMed: 19765592]

Vranken WF, Boucher W, Stevens TJ, Fogh RH, Pajon A, Llinas M, Ulrich EL, Markley JL, Ionides J, and Laue ED (2005). The CCPN data model for NMR spectroscopy: development of a software pipeline. Proteins 59, 687–696. [PubMed: 15815974]

Waibel R, Treichler H, Schaefer NG, van Staveren DR, Mundwiler S, Kunze S, Kuenzi M, Alberto R, Nuesch J, Knuth A, et al. (2008). New derivatives of vitamin B_{12} show preferential targeting of tumors. Cancer Res 68, 2904–2911. [PubMed: 18413759]

Wang R, Islam K, Liu Y, Zheng W, Tang H, Lailler N, Blum G, Deng H, and Luo M (2013). Profiling genome-wide chromatin methylation with engineered posttranslation apparatus within living cells. J. Am. Chem. Soc 735, 1048–1056.

Wang R, Zheng W, and Luo M (2014). A sensitive mass spectrum assay to characterize engineered methionine adenosyltransferases with S-alkyl methionine analogues as substrates. Anal Biochem. 450, 11–19. [PubMed: 24374249]

Wang R, Zheng W, Yu H, Deng H, and Luo M (2011). Labeling substrates of protein arginine methyltransferase with engineered enzymes and matched S-adenosyl-L-methionine analogues. J. Am. Chem. Soc. 733, 7648–7651.

Warner DF, Savvi S, Mizrahi V, and Dawes SS (2007). A riboswitch regulates expression of the coenzyme B_{12}-independent methionine synthase in *Mycobacterium tuberculosis:* implications for differential methionine synthase function in strains H37Rv and CDC1551. J. Bacteriol 189, 3655–3659. [PubMed: 17307844]

Warren MJ, Raux E, Schubert HL, and Escalante-Semerena JC (2002). The biosynthesis of adenosylcobalamin (vitamin B_{12}). Nat. Prod. Rep 19, 390–412. [PubMed: 12195810]

Watkins D, and Rosenblatt DS (2013). Lessons in biology from patients with inborn errors of vitamin B_{12} metabolism. Biochimie 95, 1019–1022. [PubMed: 23402785]

Watson E, MacNeil LT, Ritter AD, Yilmaz LS, Rosebrock AP, Caudy AA, and Walhout AJ (2014). Interspecies systems biology uncovers metabolites affecting *C. elegans* gene expression and life history traits. Cell 156, 759–770. [PubMed: 24529378]

Widner FJ, Lawrence AD, Deery E, Heldt D, Frank S, Gruber K, Wurst K, Warren MJ, and Krautler B (2016). Total synthesis, structure, and biological activity of adenosylrhodibalamin, the non-natural rhodium homologue of coenzyme B_{12}. Angew. Chem. Int. Ed 55, 11281–11286.

Winter G (2010). XIA2: an expert system for macromolecular crystallography data reduction. J. Appl. Crystallogr 43, 186–190.

Wishart DS, and Case DA (2001). Use of chemical shifts in macromolecular structure determination. Methods Enzymol 338, 3–34. [PubMed: 11460554]

Yilmaz LS, and Walhout AJ (2014). Worms, bacteria, and micronutrients: an elegant model of our diet. Trends Genet. 30, 496–503. [PubMed: 25172020]

Zaman K, and Zak Z (1989). Purification and partial characterization of a cobalamin-binding protein from chicken egg yolk. Biochim. Biophys. Acta 998, 102–104. [PubMed: 2790050]

Zayas CL, Claas K, and Escalante-Semerena JC (2007). The CbiB protein of *Salmonella enterica* is an integral membrane protein involved in the last step of the *de novo* corrin ring biosynthetic pathway. J. Bacteriol 189, 7697–7708. [PubMed: 17827296]

Highlights

- SAM analogs have been used to make variants of vitamin B_{12}
- Analogs of B_{12} with fluorescent groups attached to the corrin ring are described
- The uptake of B_{12} analogs into *E. coli* and *M. tuberculosis* is shown
- Vitamin B_{12} analogs are shown to accumulate in worms and higher plants

SIGNIFICANCE

Vitamin B_{12}, cobalamin, is an essential dietary component that is synthesized solely by certain prokaryotes. Although some eukaryotes, including mammals, require the nutrient, kingdoms such as Plantae and Fungi have evolved to live in a B_{12}-less environment, which has implications for people on a vegan diet. To follow more closely the journey undertaken by cobalamin, from its prokaryotic inception, through sharing in microbial communities and its uptake by animals, we devised ways to construct a range of fluorescent analogs of cobalamin. By manipulation of the B_{12} biosynthetic pathway we were able to modify the C5 position of the corrin framework so as to incorporate an allyl substituent, where the vinyl group could be used to attach fluorophores to give tagged cobyric acid analogs. Fluorescent cobalamin variants were also constructed through attachment of fluorophores to the ribose group in the lower nucleotide loop. Together, these fluorescent analogs were used to show that *M. tuberculosis* is able to absorb both complete and incomplete corrinoids, demonstrating that cobalamin can be used to carry cargo into the cell. *C. elegans* was also found to absorb cobalamin, demonstrating that this approach can be used to follow intracellular trafficking in a model organism. Moreover, it also represents a target for parasites such as hook worms. Finally, and very surprisingly, certain plants were observed to be able to absorb B_{12} from their growth medium, accumulating the molecule in the leaf vacuole. This latter finding may be important as a way to address the global challenge of providing a nutrient-complete vegetarian diet, a valuable development as the world becomes increasingly meat-free due to population expansion.

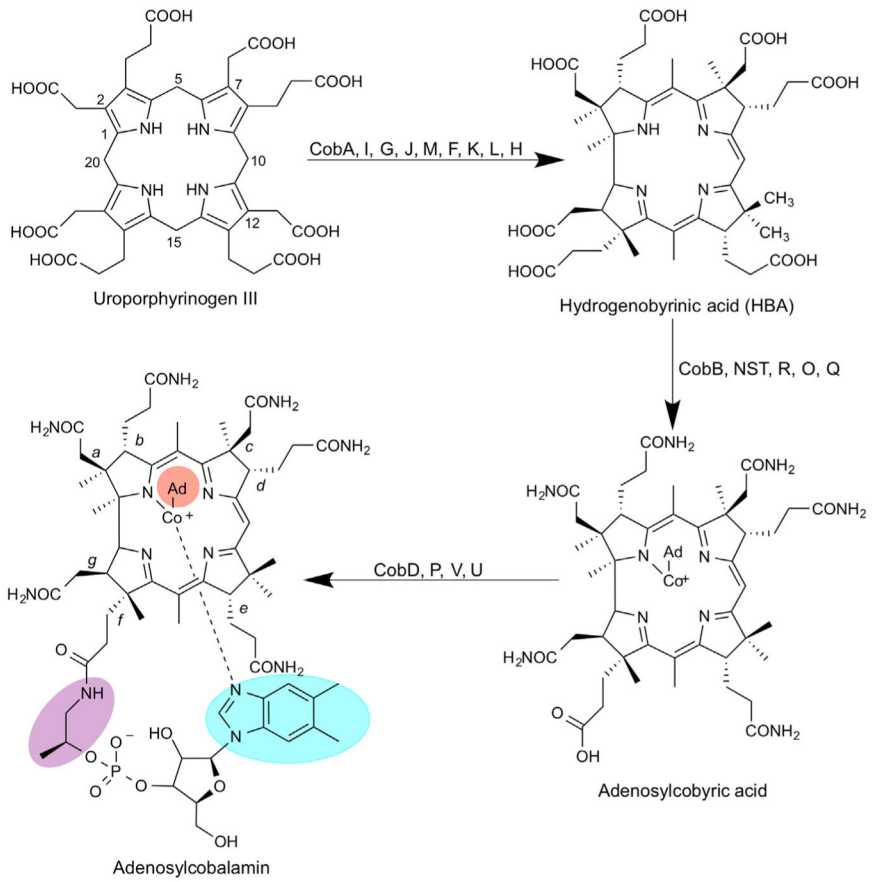

Figure 1. Biosynthesis of Adenosylcobalamin from Uroporphyrinogen III

Initially, uroporphyrinogen III is acted upon by the enzymes in the sequence of CobA, I, G, J, M, F, K, L, and H to generate a cobalt-free corrinoid called HBA. Amidation of the *a* and *c* side chains followed by metal insertion, adenosylation, and the remaining amidations by CobB, NST, R, O, and Q gives rise to adenosylcobyric acid. The final stages of the biosynthesis see the attachment of an aminopropanol side chain and the alpha ribazole nucleotide, which contains the unusual base dimethylbenzimidazole. These reactions are mediated by the enzymes CobD, P, V, and U. The numbering of the corrin macrocyle (1–20) is shown as is the lettering associated with the side chains (*a*-*g*). Different variants of cobalamin are found through changes in the highlighted areas of the molecule. The upper ligand (orange) can be a methyl, cyano, or water group, the linking aminopropanol (purple) is an ethanolamine molecule in nor-cobalamin, and a range of different bases can replace the dimethylbenzimidazole (blue).

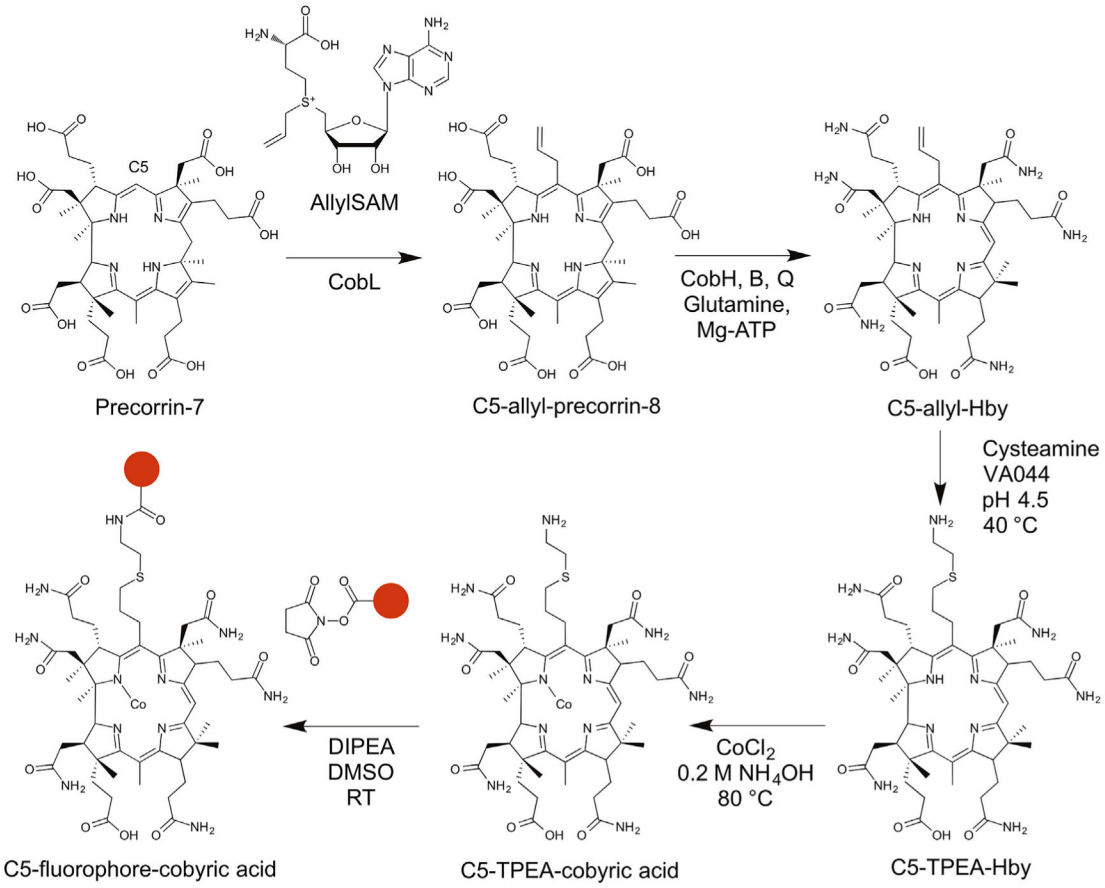

Figure 2. The ChemBio Synthesis of a C5 Analog of Cobyric Acid

Precorrin-7 is modified with an allyl-SAM derivative by the action of the C5 methyltransferase, CobL. This results in the production of C5-allyl-precorrin-8, which is acted upon by the enzyme CobH, B, and Q to generate C5-allyl-Hby. Cysteamine is next chemically attached to the allyl group to generate C5-(TPEA)-Hby prior to the chemical insertion of cobalt to give C5-(TPEA)-cobyric acid. The coupling of a fluorophore via the free amine group on C5 generates the C5-fluorophore conjugate of cobyric acid. The fluorophore is represented by the filled red circles.

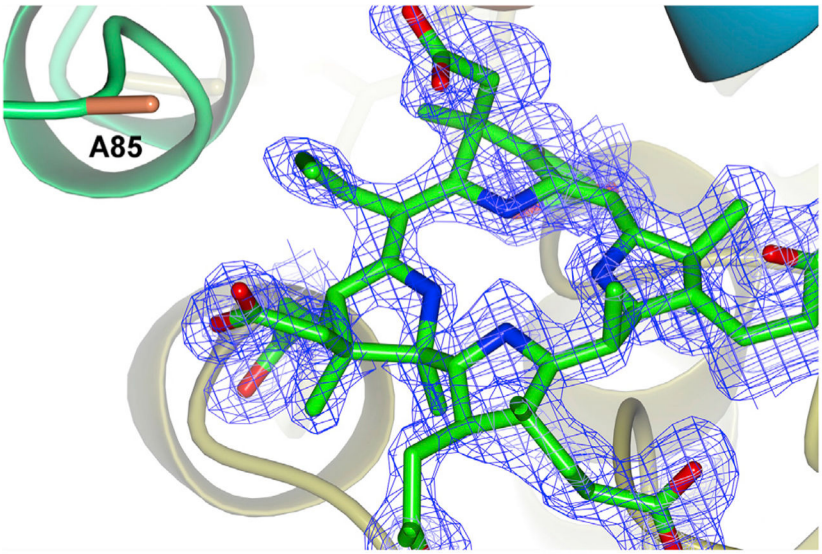

Figure 3. Product Complex of CobH^{T85A} with C5-allyl-HBA

The figure shows the position of the reaction product bound at the active site of the enzyme. The proximity of the C5 group to Ala85 demonstrates how the removal of the threonine side chain has provided extra space to accommodate the allyl group.

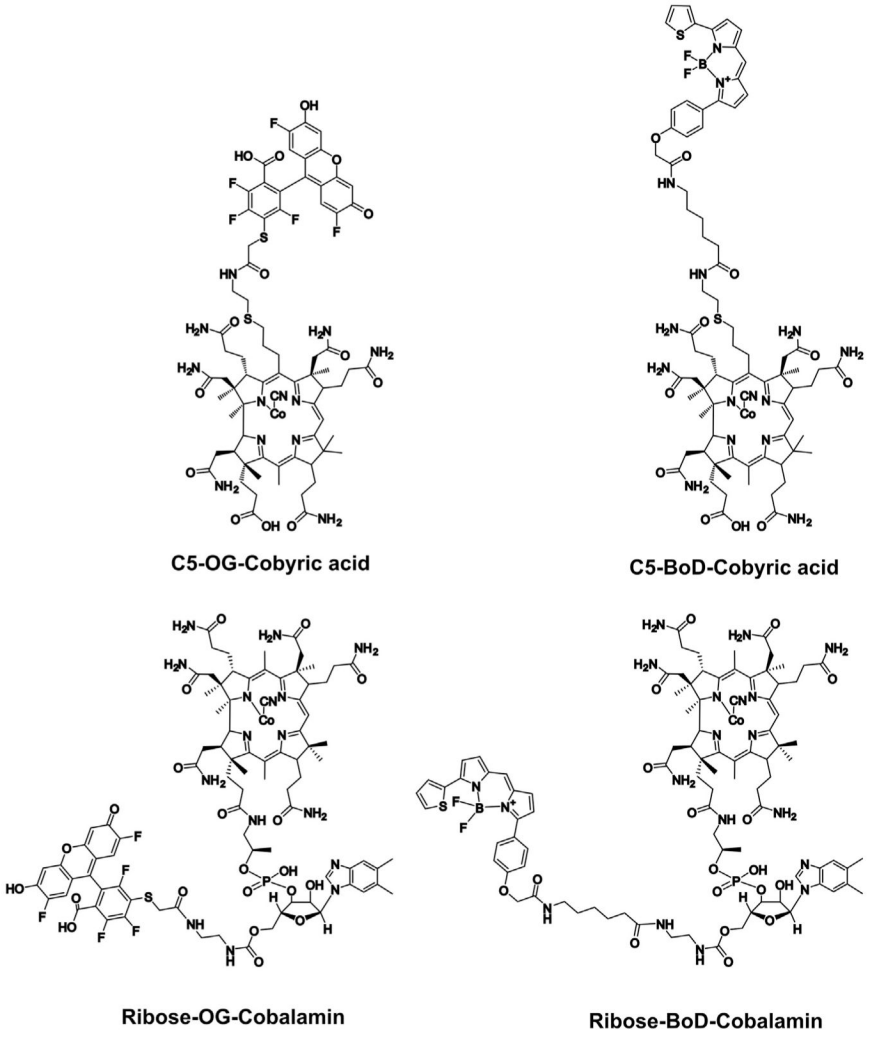

Figure 4. Chemical Structures of the Four Fluorescent Analogs of Cobalamin

The top two structures show the attachment of Orgeon green (GO) and BoDIPY (BoD) to the C5 position of the corrin ring, whereas the lower two structures show how these fluorophores are attached to the ribose moiety of the lower nucleotide loop.

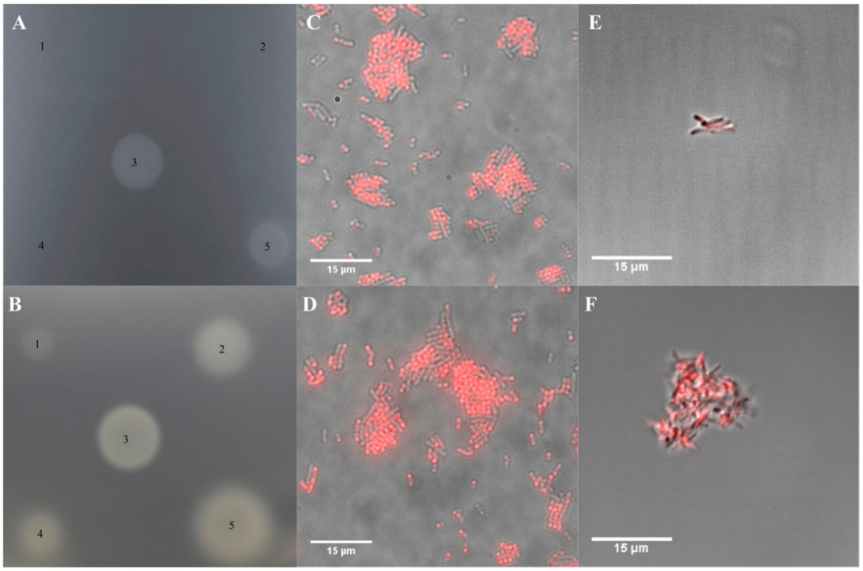

Figure 5. Effect of Cobyric Acid and Cobalamin Analogs on Bacteria

(A) A bioassay plate containing an *S. enterics* strain that requires cobyric acid or later pathway intermediates for growth. Addition of a known amount of vitamin B_{12} (spot 3) allows growth. Spots 1, 2, and 4 represent C5-allyl-hydrogenobyrinic acid *a,c*-diamide (C5-allyl-HBAD), C5-allyl-Hby, and C5-(TPEA)-Hby, none of which promote growth. Spot 5 contains the C5-(TPEA)-cobyric acid analog and promotes growth.

(B) The same bioassay plate assay as in (A), with spot 3 containing a standard vitamin B_{12} solution. Spots 1, 2, 4, and 5 are solutions of C5-BoD-co-byricacid, ribose-BoD-cobalamin, C5-OG-cobyric acid, and ribose-OG-cobalamin, respectively. All the analogs support growth although the C5 analogs are weaker than the respective ribose-linked analogs.

(C and D) Overlay pictures of *E. coli* cells that have been grown in the presence of ribose-BoD-cobalamin and C5-BoD-cobyric acid, respectively. The co-localization of the red fluorescence with the cells indicates that *E. coli* has taken up both compounds.

(E and F) Cultures of *M. tuberculosis*, grown in the presence of ribose-BoD-cobalamin and C5-BoD-cobyric acid, respectively. Again, the presence of the red fluorescence with the cells indicates that *M. tuberculosis* is able to take up both analogs.

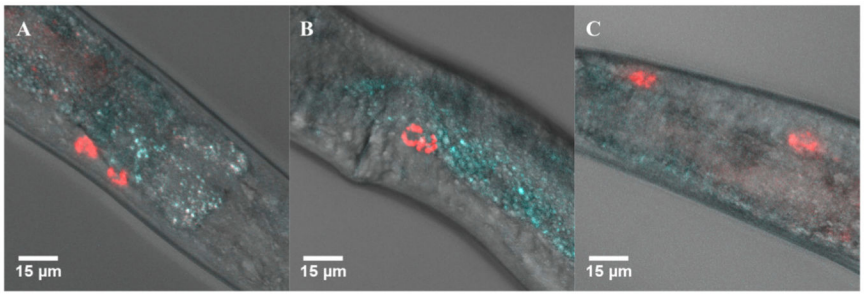

Figure 6. Localization of Ribose-BoD-Cobalamin to Coelomocytes in *C. elegans*

(A–C) *C. elegans* were fed with *E. coli* OP50 that had been grown in the presence of ribose-BoD-cobalamin and were imaged after several days. The red fluorescence associated with the fluorophore was found localized in the six coelomocytes, two of which are found at the head (A), two near the vulva (B) and two at the anus (C).

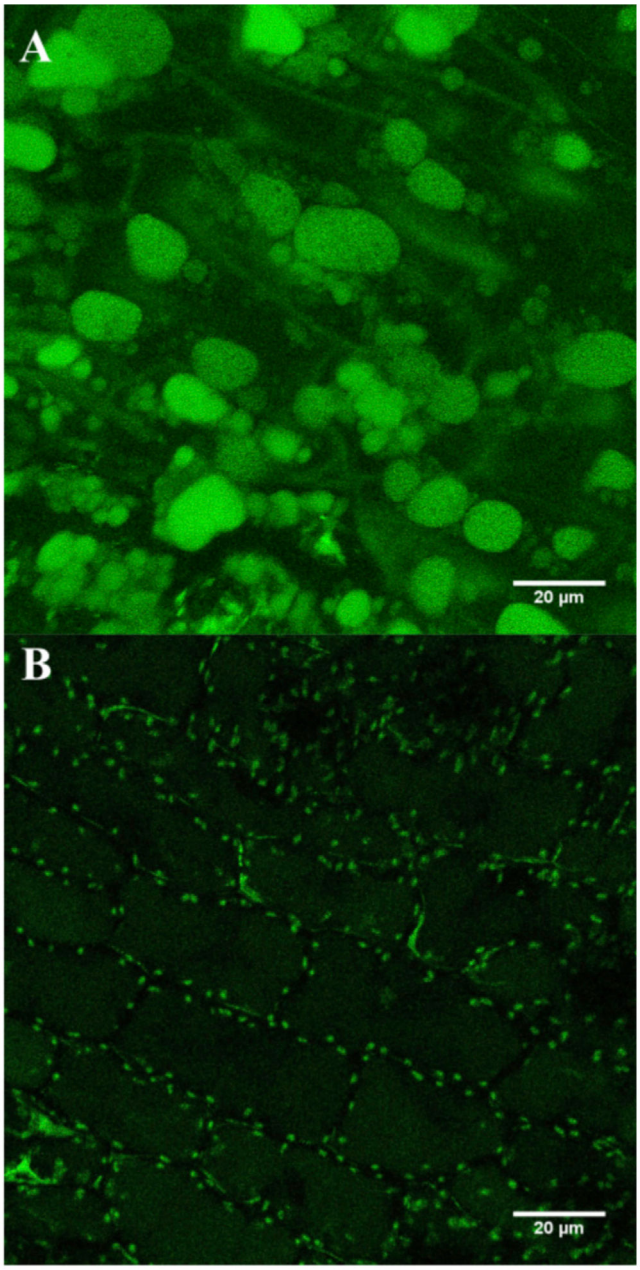

Figure 7. Localization of Ribose-OG-Cobalamin to Vacuoles in *L. sativum* (Garden Cress)

(A and B) Seeds were germinated in sterile media containing ribose-OG-cobalamin and were imaged after 5 days. Thin sections of the cotyledons of cress grown in the presence of the ribose-OG-cobalamin had highly fluorescent vacuoles (A), whereas control plants grown in the absence of the cobalamin derivative lacked this fluorescence (B).

KEY RESOURCES TABLE

REAGENT or RESOURCE	SOURCE	IDENTIFIER
Bacterial and Virus Strains		
E. coli: JM109 *end*A1 *rec*A1 *gyr*A96, *thi hsd*R17 (r_κ-m_κ^+) *rel*A1 *sup*E44 Δ(*lac-pro*AB) [F', *tra*D36 *pro*AB *lac*I^{q}ZΔM15]	Promega	JM109
E. coli: BL21(DE3) pLysS F$^-$ *ompT hsdS*$_B$ (r_B^-, m_B^-) *gal dcm* (DE3) pLysS (Cm^R)	Novagen	BL21(DE3) pLysS
E. coli: BL21(DE3) F$^-$ *ompT hsdS*$_B$ (r_B^-, m_B^-) *gal dcm* (DE3)	Novagen	BL21(DE3)
E. coli: Rosetta (DE3) F$^-$ *ompT hsdS*$_B$(r_B^-, m_B^-) *gal dcm* (DE3) pRARE (Cam^R)	Novagen	Rosetta (DE3)
E. coli: OP50 Uracil auxotroph	Gift from J. Tullet	N/A
E. coli: OP50 (pET-BAD-*btuBF*)	This paper	N/A
E. coli: OP50 (pET 3a)	This paper	N/A
M. tuberculosis: H37Rv ATCC® 27294	Gift from H. Boshoff	N/A
M. tuberculosis: H37RvJO	Gift from H. Boshoff	N/A
M. tuberculosis: *ΔbacA* H37RvJO with *hyg*-marked *ΔbacA* deletion	Warner et al., 2007; Gopinath et al., 2013a, 2013b)	N/A
M. tuberculosis: *ΔmetE* H37RvJO with *hyg*-marked *ΔmetE* deletion.	Warner et al., 2007; Gopinath et al., 2013a, 2013b)	N/A
M. tuberculosis: *ΔmetH* H37RvJO with *ΔmetH* deletion.	Warner et al., 2007; Gopinath et al., 2013a, 2013b)	N/A
S. enterica: AR3612; *cysG, metE*	(Raux et al., 1996)	N/A
Chemicals, Peptides, and Recombinant Proteins		
S-(5'-Adenosyl)-L-homocysteine	Sigma	Cat# A9384
Allyl-bromide	Sigma	Cat# A29585
Silver perchlorate	Sigma	Cat# 674583
Adenosine 5′-triphosphate disodium salt hydrate	Sigma	Cat# A2383
L-Glutamine	Sigma	Cat# G3126
Lichroprep RP18	VWR	Cat# 1.09303.0500
Diethylaminoethyl–Sephacel® aqueous ethanol suspension	Sigma	Cat# I6505
Cysteamine hydrochloride	Sigma	Cat# M6500
VA-044 2,2'-Azobis[2-(2-imidazolin-2-yl)propane] Dihydrochloride, Water Soluble Azo Initiator	Alpha Laboratories	Cat# 017–19362
BODIPY® TR-X NHS Ester (Succinimidyl Ester)	ThermoFisher	Cat# D-6116

REAGENT or RESOURCE	SOURCE	IDENTIFIER
Oregon Green® 514 Carboxylic Acid, Succinimidyl Ester	ThermoFisher	Cat# O-6139
Porpargyl bromide solution	Sigma	Cat# 81831
Seleno-L-methionine	Sigma	Cat# S3132
CobL	(Deery et al., 2012)	N/A
CobH	(Deery et al., 2012)	N/A
CobB	(Deery et al., 2012)	N/A
CobQ^{Alv}	This paper	N/A
BtuF	(Deery et al., 2012)	N/A
CobH (T85A)	This paper	N/A
hMAT2A (I117A)	Gift from U. Oppermann (Oxford)	N/A
SAHH	Gift from J. Micklefield (Manchester)	N/A
Molecular dimensions Structure Screen 1	Molecular dimensions	Cat# MD1–01
Deposited Data		
Structure of *R. capsulatus* CobH (T85A) in complex with C5-allyl-HBA.	This paper	PDB: 5NOG
Experimental Models: Organisms/Strains		
N2 *C. elegans*	Gift from J. Tullet (Kent)	N/A
A. thaliana	Gift from A. Smith (Cambridge)	N/A
L. sativum	Meadow Grange Nursery, Blean.	N/A
Oligonucleotides		
Allochromatium vinosum CobQ Forward: CTACATATGACCGATTCAGCCCCCAC	This paper	N/A
Allochromatium vinosum CobQ Reverse: CATACTAGTTCAGCGTGCCAGTTCGAG	This paper	N/A
R. capsulatus CobH (T85A) Forward:	This paper	N/A
R. capsulatus CobH (T85A) Reverse:	This paper	N/A
Recombinant DNA		
pET14b	Novagen	Cat# 69660
pET3a	Novagen	Cat# 69418-3
pLysS	Novagen	Cat# 69659-3
pETcoco-2	Novagen	Cat# 71148-3
pET3a-*cobAIGJFMKL*^{C}*E*^{His}	(Deery et al., 2012)	N/A
pET14b-*cobL*	(Deery et al., 2012)	N/A
pET14b-*cobH*	(Deery et al., 2012)	N/A
pET14b-*cobB*	(Deery et al., 2012)	N/A
pET14b-*cobQ*	This paper	N/A

REAGENT or RESOURCE	SOURCE	IDENTIFIER
pET14b-*btuF*	(Deery et al., 2012)	N/A
pLysS-*btuB*	(Deery et al., 2012)	N/A
pET14b-*cobH*(T85A)	This paper	N/A
pET14b-*hMat2A*(I117A)	This paper	N/A
pET28-*SAHH*	Gift from J. Micklefield (Manchester)	N/A
Software and Algorithms		
Coot	(Emsley et al., 2010)	https://www2.mrc-lmb.cam.ac.uk/personal/pemsley/coot/
XIA2 version 0.3.8.0	(Winter, 2010)	https://xia2.github.io
CCP4i	(Potterton et al., 2003)	http://www.ccp4.ac.uk/ccp4i_main.php
CCPN analysis	(Vranken et al., 2005)	http://www.ccpn.ac.uk/v2-software/software/analysis